

## ANALYSIS OF PROGRESSIVE COLLAPSE OF A SUPER-LONG SPAN LATTICED STEEL ARCH STRUCTURE

SHUANGCHAO GUO, DELIN XU, KAIGUANG SHANG, SHUO YANG, DI WANG, GEN LI  
*Beijing Construction Engineering Group Co., Ltd, Beijing, China*

BING ZHENG

*Department of Civil Engineering, China Agricultural University, Beijing, China*

YONG JIAO

*Beijing Construction Engineering Group Co., Ltd, Beijing, China*

*e-mail: jy701210@sina.com*

The progressive collapse of a space grid structure which has a large number of members and a large span is the focus of current research. Before the progressive collapse of the structure, there is a problem of instability of the members. In this paper, dynamic nonlinear analysis of a super-long span latticed steel arch structure is carried out to study its progressive collapse process using a Kinematic Hardening Plasticity constitutive model compiled by Vumat material subprogram in Abaqus, which takes into account instability of the members. Differences in the dynamic response process of the structure at the collapse moment and the failure sequence of the members using the member stability model and the material failure constitutive model are compared. Compared with the material failure constitutive model, when the member stability constitutive model is used, the proportion of compressive buckling members in the structural failure is higher, and the bearing capacity of the structure is lower when the initial failure occurs. The structure suffers from localized member compressive failure rather than material yielding, which leads to the progressive collapse of the structure.

*Keywords:* progressive collapse, steel arch truss structure, compression instability

### 1. Introduction

The steel arch truss structure, as one of the common forms of space grid structures, combines the advantages of arch and truss, light self-weight, large span, good force performance and short construction period, which make it to be widely used in large-span public buildings such as stadiums, terminals and industrial plants (Zhu *et al.*, 2013; Cai *et al.*, 2010; Zhao and Wu, 2016). The progressive collapse of such large public buildings will pose a great threat to people's life safety and public property once it occurs. The traditional concept believes that the spatial grid structure itself has a high degree of redundancy, thus not collapsing on a large scale. In 1978, the overall collapse and damage of a stadium with a quadrangular pyramid grid system in the center of Hartford City in the United States occurred in a heavy snowstorm, which aroused the attention of domestic and foreign scholars to the progressive collapse of space grid structures (Jiang and Chen, 2012).

Progressive collapse is a process of overall collapse or disproportionate large-scale collapse caused by local failure of the structure (GB50068, 2018). The research on the progressive collapse resistance of structures has been going on for more than 40 years. At present, the research on the progressive collapse resistance of frame structures (Song and Sezen, 2013; Zhang, 2013; Koh and Krauthammer, 2019; Wang and Wang, 2021) and truss structures (Zhao *et al.*, 2019; Miyachi *et al.*, 2012) is relatively mature, and the research focus is shifting to large-span space structures.

For space grid structures, the occurrence of progressive collapse is mainly caused by stability failure of compression members and strength failure of the node zone (Tian *et al.*, 2019). The failure of members is the key to structural design, which can be divided into two types: strength failure and instability failure. The ultimate bearing capacity of the instability failure, generally occurring in compression members, is far less than the yield strength of the strength failure, generally occurring in tension members. Before the overall failure of the space grid structure, there will be a problem of instability of the members, hence finding the key members is an important problem in analysis of the progressive collapse of the structure. The transformed load path method is the most commonly used analysis method to study the progressive collapse of space structures. Tian *et al.* (2019) proposed a dynamic analysis method to simulate the progressive collapse of large-span spatial lattice structures, and analyzed the progressive collapse resistance mechanism of large-span single-story spatial lattice structures. By assuming failure of some key members, the structure is analyzed to determine whether a new load transfer path can be formed and thus whether the progressive collapse of the structure will occur. For the purpose of considering the instability of the member, some scholars use the Vumat subprogram provided by Abaqus to compile the constitutive model of the member, and use the self-defined failure criterion of the member to find the key member (Ding *et al.*, 2011; Ge, 2012). Wilkes and Krauthammer (2019) proposed a method based on energy flow to analyze failure members in a structure. Han *et al.* (2018) identified two forms of collapse of the grid structure through the displacement criterion and found the key members based on the sensitivity method. Han *et al.* (2021) used a transformed load path method to analyze the progressive collapse performance of a single layer latticed shell structure and determined the effect of key members and member groups on the progressive collapse resistance of the structure.

At present, the research on progressive collapse performance of space grid structures is mainly focused on single-layer or double-layer latticed shell structures, and the analysis on truss structures is mainly focused on a plane truss, relatively less than a spatial truss. It should be highlighted that most of Vumat subprograms are only available for pipe section members, while the constitutive model compiled by the Vumat subprogram used in this paper can be applied to arbitrary sections, taking into account instability of the member. The force status of the member is monitored by the subprogram and the failure member is removed in real time, making it easier to find the location of key members. In this paper, an explicit dynamic calculation method for a super-long span space steel arch truss structure is conducted to study the difference between the material failure constitutive model and the member stability constitutive model compiled by the Vumat subprogram in progressive collapse analysis of the structure, verifying the feasibility of the Kinematic Hardening Plasticity constitutive model compiled by the Vumat subprogram in practical engineering applications.

## 2. Materials and methods

### 2.1. Model information

The model is based on a super-long span latticed steel arch structure divided into two parts and arranged symmetrically. Its plane size is 211 m×460 m and the height is about 60 m. A total of 32 main trusses are arranged longitudinally with a distance of 15 m, and each part has 16 trusses. The main spatial arch truss has an inverted triangle section, width of 4 m and variable height from 5.5 m to 7 m. Seven connecting trusses and a number of spaced cross struts are arranged between the main trusses to ensure the out-of-plane stability of the main truss. The arch curve is a three-center circular arch with height of about 60 m, forming an inverted quadrangular pyramid space arch truss structure system with a rise-to-span ratio of 0.28. Figure 1 plots the top view of half of the arch truss model that has been established in Abaqus. In order

to describe the instability of the members during progressive collapse of the model more clearly, the key positions of the first truss on both sides have been marked with I-IV in the structure top view.

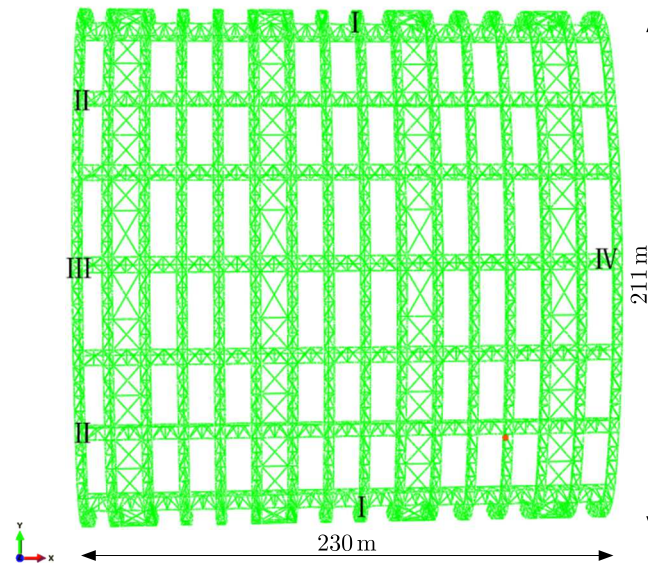


Fig. 1. Top view of the model

## 2.2. Material performance and section type

Section types of the simplified model members are all steel pipe, and the section materials are all Q345 steel whose main material parameters are shown in Table 1.

**Table 1.** Material parameter

Yield stress $f_y$	Elastic modulus $E$	Density $\rho$	Poisson's ratio $\nu$	Breaking strain
345 MPa	206 GPa	7850 kg/m <sup>3</sup>	0.3	0.02

The members are mainly divided into the upper chord, lower chord and web member according to their positions in the truss. Table 2 is a summary of the member section types used in different parts of the structure, where  $\emptyset$  represents pipe section, the former number and the latter one represent the outer radius and thickness of the pipe section, respectively.

**Table 2.** Section types of the members

Member parts	Section type
Upper and lower chord	$\emptyset 560 \times 25$ , $\emptyset 500 \times 24$ , $\emptyset 450 \times 24$ , $\emptyset 400 \times 24$ , $\emptyset 377 \times 20$ , $\emptyset 351 \times 18$ , $\emptyset 351 \times 16$ , $\emptyset 325 \times 16$ , $\emptyset 299 \times 14$ , $\emptyset 273 \times 14$ , $\emptyset 273 \times 10$ , $\emptyset 245 \times 12$
Web members	$\emptyset 245 \times 12$ , $\emptyset 219 \times 10$ , $\emptyset 219 \times 8$ , $\emptyset 194 \times 8$ , $\emptyset 180 \times 8$ , $\emptyset 159 \times 6$ , $\emptyset 140 \times 5$ , $\emptyset 114 \times 4$ , $\emptyset 89 \times 4$

## 2.3. The constitutive model

In this paper, two constitutive models are employed to study progressive collapse performance of the arch truss structure considering compression instability of the members. The first one is the material failure constitutive model which applies material failure as the failure criterion for

element members. As Q345 steel is adopted, the stress-strain curve of Q345 steel is simplified to a two-stage folding line for simplified model calculation. When the compressive and tensile stresses of the members reach the yield stress, the modulus of elasticity of the member is reduced by 0.01 times of the original value. The ultimate strain of Q345 steel is 0.025, and when the material strain is close to the ultimate strain, the maximum stress and strain fluctuate less and have less influence on the calculation results. The member is determined to fail when strain of the member exceeds the failure strain of the material which is set to 0.02 in this paper. The stiffness change of the material at different stress stages is described by multiplying the elastic modulus by different coefficients  $k$ , that is,  $E' = kE$ . The stress-strain equations of the material failure constitutive model is given in Eq. (2.1), where  $\varepsilon_y$  represents the strain at which the member stress reaches the yield strength  $f_y$ . In the process on progressive collapse of the space grid structure, slender compression members are peculiarly prone to buckling and tend to fail before reaching the yield load, making the actual bearing capacity of the member lower

$$k = \begin{cases} 1 & \text{for } -\varepsilon_y \leq \varepsilon \leq \varepsilon_y \\ 0.01 & \text{for } |\varepsilon| > \varepsilon_y \end{cases} \quad (2.1)$$

Vumat is a program interface provided by Abaqus finite element software for users to compile self-defined materials. The second one is based on the Vumat subprogram in Abaqus to develop a Kinematic Hardening Plasticity constitutive model considering compression instability of members. This model introduces the Marshall model and the stability coefficient of the compressed member. The Marshall model (Marshall *et al.*, 1977) is based on the hysteresis curve obtained from a steel circular tube test, which describes the hysteresis performance of an inelastic member containing initial defects and a decrease of axial stiffness after compression instability. The model is optimized on the basis of the Marshall model, and the stress-strain curve of the optimized model is shown in Fig. 2. The optimized model consists of several straight lines, indicating that the elastic modulus of the member differs at different stages. When the axial strain of the member, represented by the  $X$ -axis, is greater than 0, the member is in tension. The stiffness change of the material at different stress stages is described by multiplying the elastic modulus of the material by different coefficients  $k$ , that is  $E' = kE$

$$k = \begin{cases} 0.01 & \text{for } \varepsilon > \varepsilon_y \\ 1 & \text{for } \varepsilon_{cr} \leq \varepsilon \leq \varepsilon_y \\ \alpha & \text{for } \varepsilon' \leq \varepsilon < \varepsilon_{cr} \\ \beta & \text{for } \varepsilon < \varepsilon' \end{cases} \quad (2.2)$$

where  $\varepsilon_{cr}$  represents the strain at which the stress reaches the yield strength  $P_{cr}$ .  $P_{cr}$  represents the critical stress when instability of the compression member occurs, calculated by the stability coefficient  $\varphi$  of the compression member in the Standard for Design of Steel Structures (GB50017-2017), that is  $P_{cr} = \varphi f_y$ .  $\varphi$  is calculated according to parameters such as section type, length, elastic modulus and radius of gyration of the member, and the physical meaning of critical control point  $\varphi$  is the same as the stability coefficient of pressure brace in the Standard for Design of Steel Structures. When the compressive stress of the member exceeds the compressive instability critical stress  $P_{cr}$  of the member, the axial stiffness will decrease.  $\alpha$  and  $\beta$  represent the initial weakening coefficient of the elastic modulus and the deep weakening coefficient of stiffness after instability of the compression member occurs, respectively.  $\varepsilon'$  represents the critical strain at the initial weakening and deep weakening of the elastic modulus of the member. The calculation formula is as follows

$$\varepsilon' = \varepsilon_{cr} - \frac{(1 - \gamma)\sigma_{cr}}{-\alpha E} \quad (2.3)$$

where  $\alpha$ ,  $\beta$ ,  $\gamma$  are coefficients summed up from the hysteresis curve of the steel round tube test, and the values in this model are as follows

$$\alpha = 0.13 \quad \beta = 0.02 \quad \gamma = 0.28$$

$\sigma_u$ ,  $\varepsilon_u$  are the stress and strain when the member is unloaded under compression, and the calculation formula for  $k$  is as follows

$$k = \frac{\sigma_y - \sigma_u}{\varepsilon_y - \varepsilon_u} \quad (2.4)$$

When strain of the member reaches point  $D$ , which is the failure strain of the member, it indicates that the member has completely lost its bearing capacity. At this time, it is determined that the member is failed and then deleted.

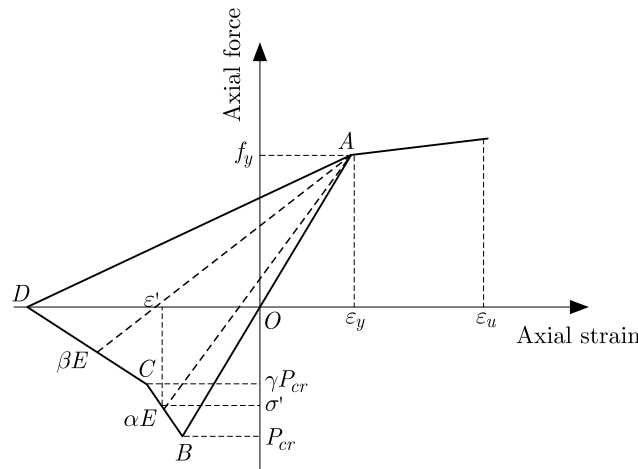


Fig. 2. Member-stabilized constitutive model

In order to introduce this model into the subprogram, some important material parameters need to be defined. Table 3 shows description of the main material parameters in the Vumat subprogram, and these nine parameters need to be added in the Abaqus user-defined material. With the input material parameters, the subprogram will automatically calculate the compression instability critical pressure  $P_{cr}$  and other related parameters of each member. The Vumat subprogram monitors the stress state of the members and updates parameters like the elastic modulus in real time by using the feature of transferring specific variables with the main program at the beginning and end of each incremental step, which simulates member stiffness degradation. The strain of the member is also used as an indicator to determine failure of the member. When the member is in compression, the failure is judged when the strain is greater than the D point, and when the member is in tension, the failure is judged when the strain is greater than the ultimate strain.

When using the Vumat subprogram, Abaqus cannot automatically calculate the transverse shear stiffness of the section, and the user needs to define and input the transverse shear stiffness  $K_{23}$  and  $K_{13}$  of the section. The calculation formula for the shear stiffness of the beam section is as follows

$$K_{13} = K_{23} = mGA \quad G = \frac{E}{2(1 + \nu)}$$

where  $G$  is the shear modulus,  $A$  is the cross-sectional area and  $m$  is the shear non-uniformity coefficient of the section, which is selected according to the section category (parameter 9) in Table 1. When the section type is circular, take 0.89.

**Table 3.** Vumat main parameters

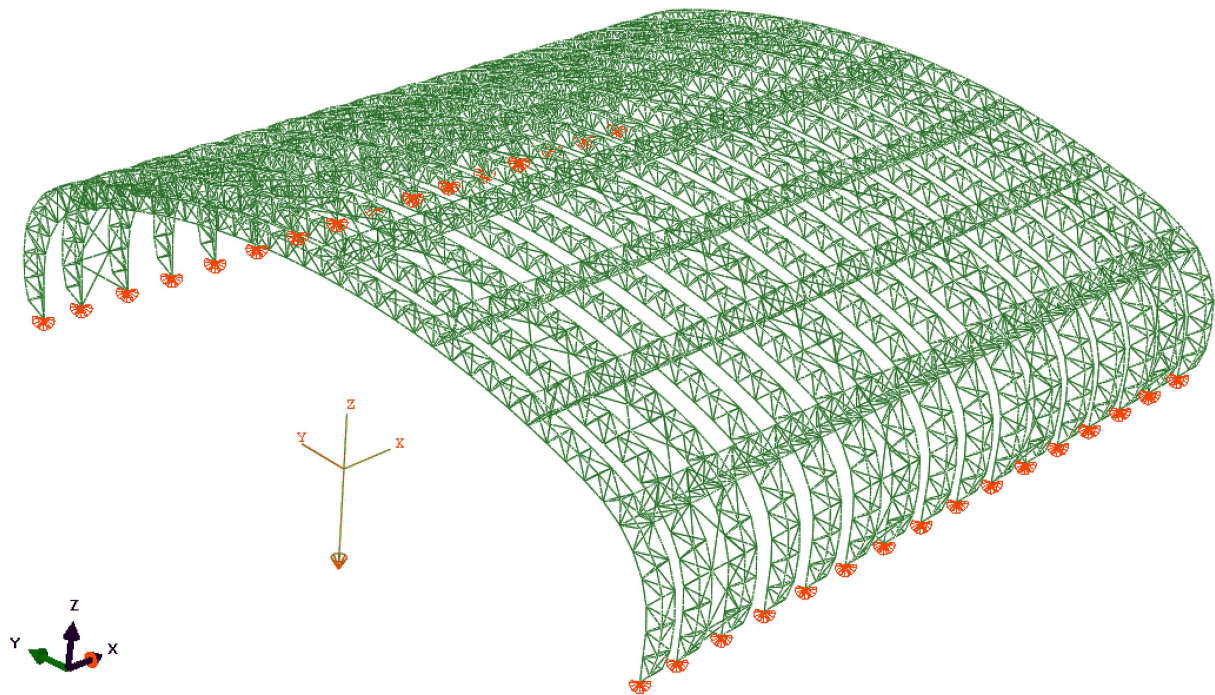
Material parameters	Illustrate
1	Elastic modulus
2	Poisson's ratio
3	Yield strength
4	Weak axis radius of inertia
5	Hardening factor (0.01)
6	Marshall simplified model parameter $\alpha(-0.13)$
7	Marshall simplified model parameter $\beta(-0.02)$
8	Marshall simplified model parameter $\gamma(0.28)$
9	Section category (1)

#### 2.4. Load

The explicit module of Abaqus is employed to simulate the progressive collapse process of the calculation structure, and only a dynamic display analysis step with a time length of 4 s is added. To simulate the load condition of the upper part of the steel arch truss structure, 5 times gravity load ( $49 \text{ m/s}^2$ ) is added along the  $z$ -direction, which increases linearly to the maximum value in the first 2 s, and remains constant in the last 2 s so as to avoid oscillations in the results. The load amplitude curve is shown in Table 4.

**Table 4.** Load amplitude

Time/frequency	Amplitude
0	0
2	1
4	1

**Fig. 3.** Constraints and loads

The supports on both sides of the structure are all hinged. The displacement of nodes in  $x$ ,  $y$  and  $z$  directions are constrained. Figure 3 shows the constraint position and load application direction of the structure.

## 2.5. Structural failure criterion

At present, there are many failure criteria for determining structure collapse. Displacement criteria are applied in this paper to determine whether progressive collapse occurs. When the vertical displacement of the structural node exceeds  $1/50$  of the span, it is considered that the structure has collapsed. The maximum span of this structure is 211 m, hence when the maximum vertical displacement of the structure exceeds 4.2 m, the collapse of the structure is judged.

## 3. Analyses and results

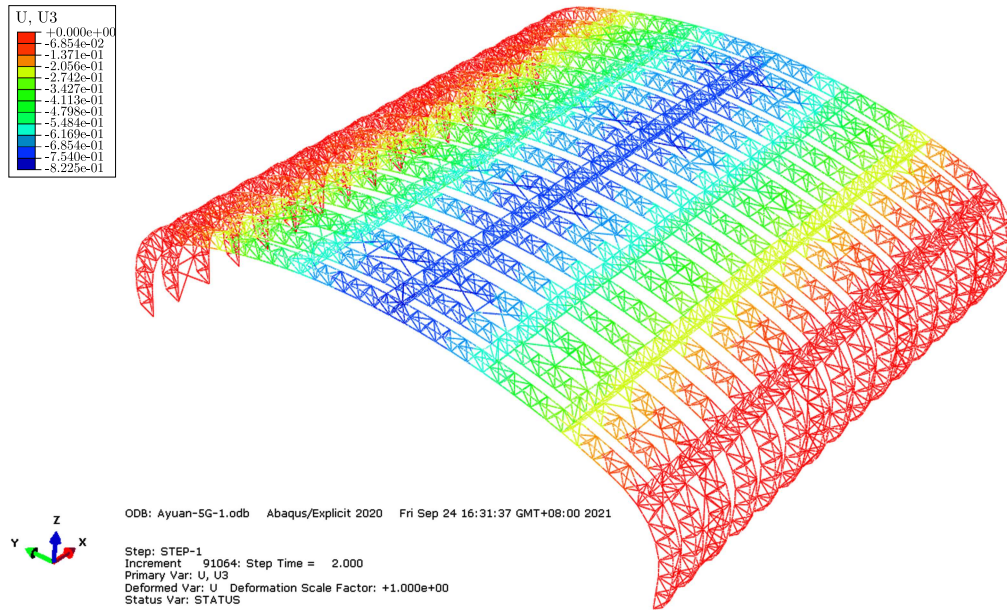
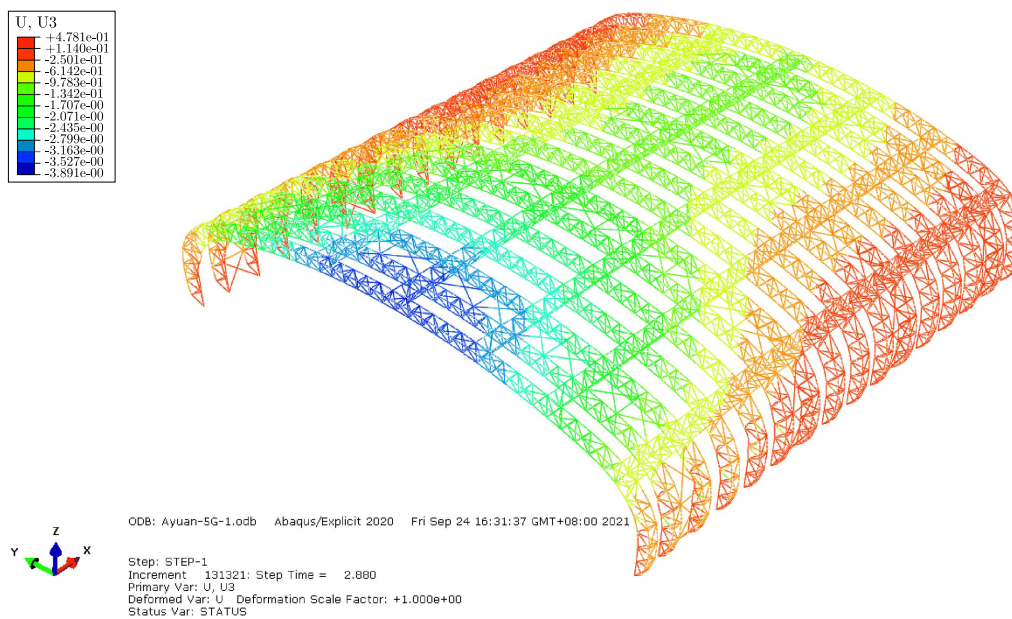
### 3.1. The material failure constitutive model

#### 3.1.1. Vertical displacement of the structure

Figures 4-8 are displacement diagrams at different times when the material failure constitutive model is used for progressive collapse analysis. In Figs. 5-11, positions of failed members at different times are marked with red circles. Figure 4 shows the displacement diagram of the structure at  $t = 2.0$  s, which is the moment when all loads are applied to the structure. It can be seen that the vertical displacement is basically symmetrically distributed along the central axis of the main truss. The vertical displacement of the middle zone of the truss is larger than that of the two sides. Figure 5 shows the displacement at  $t = 2.9$  s, when the first failure member appears, the maximum vertical displacement of the structure reaches 3.891 m, which does not exceed  $1/50$  of the span. Figure 6 shows the displacement at  $t = 3.0$  s, after the member failure, the vertical displacement increases rapidly, the maximum node displacement is 6.34 m, which exceeds  $1/50$  of the span, and the collapse of the structure is judged. Figures 7 and 8 display displacement diagrams of the structure at different angles at  $t = 4.0$  s. It can be found that during the whole process from the beginning of loading to the end, the vertical displacement of zone III is larger than that of other positions. The maximum displacement point appears at the mid-span position of the first truss, on the left in Fig. 8. When  $t = 4.0$  s, the maximum nodal displacement of the structure reaches 57.43 m, leading to serious overall deformation of the structure. In Fig. 7, zone I and III are the most severely damaged, and the structure failure occurs basically.

#### 3.1.2. Member failure order

At  $t = 2.0$  s, the structural load reaches the maximum value, and there is no failure member in the structure. At  $t = 2.9$  s, the first failure member appears at the marked position of zone III in Fig. 5, which is the upper chord of the truss, and the failure form is compression failure. It can be seen from Fig. 6 that during the time from 2.880 s to 3.000 s, with the position of the first failure member as the center, spreading along the direction of the connecting truss, more failure members appear in the adjacent positions. Meanwhile, a part of the trusses in zone I has failure members, all of which are the upper chords of the truss, and the failure mode is tensile failure. It can be seen from Fig. 7 that during the time from 3.0 s to 4.0 s, due to influence of the internal force redistribution of the structure, the load originally borne by the failure member is transferred to the surrounding members, and a large number of failure members appear, thus resulting in further structural damage. It is worth noting that the locations of failure members are mainly concentrated in zone I and III. Most of the failure members in zone I are the upper

Fig. 4. Structure displacement diagram,  $t = 2.0$  sFig. 5. Structure displacement diagram,  $t = 2.9$  s

chord members of the truss, and a small part contains diagonal web members. At first, only a few upper chords of the trusses are damaged by tension, and finally the upper chords of all trusses in the same position are damaged. Zone III is the one where the failure member occurs first, with the largest vertical displacement of the structure. After the first failure member appears, other failure members spread from zone III to zone IV. In general, the largest number of failure members and the most serious structural damage lie in zone III.



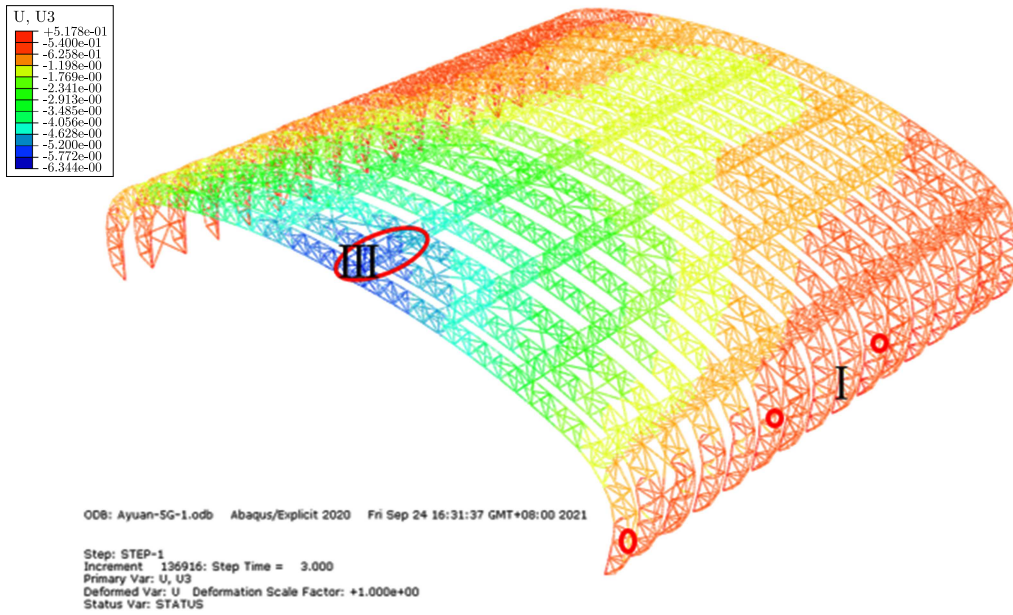


Fig. 6. Structure displacement diagram,  $t = 3.0$  s

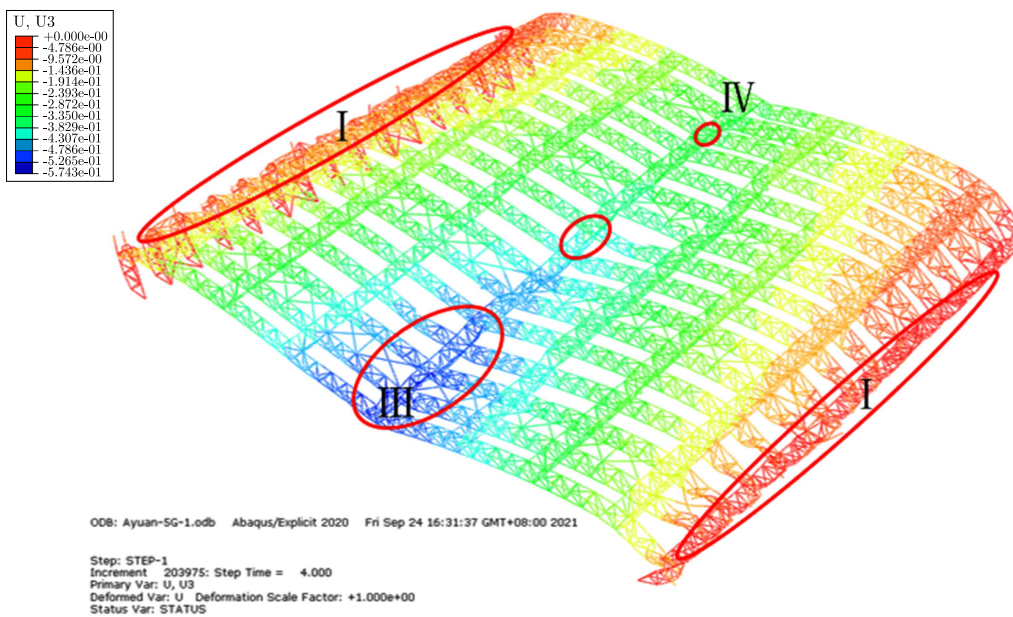


Fig. 7. Structure displacement diagram,  $t = 4.0$  s

### 3.2. Member-stabilized constitutive model

#### 3.2.1. Vertical displacement of the structure

The displacement process at different times with the member stability constitutive model is shown in Figs. 9-12. Figure 9 depicts the displacement of the structure at  $t = 1.32$  s, which is the moment when the first instable member appears in the structure. It can be seen from the figure that the overall vertical displacement distribution of the structure at the moment of initial loading is basically consistent with Fig. 4, with the vertical displacement in the middle of the truss being larger and gradually decreasing to both sides. As can be seen from Fig. 10, the maximum nodal vertical displacement of the structure is 4.52 m, which exceeds 1/50 of the span of the structure at  $t = 1.76$  s, at this time the structure has collapsed. The displacement diagram

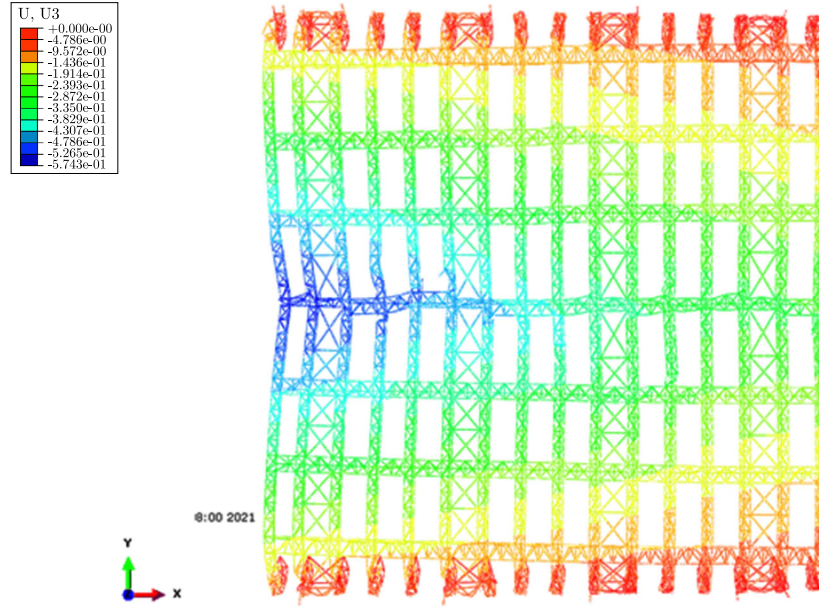


Fig. 8. Top view of structure,  $t = 4.0$  s

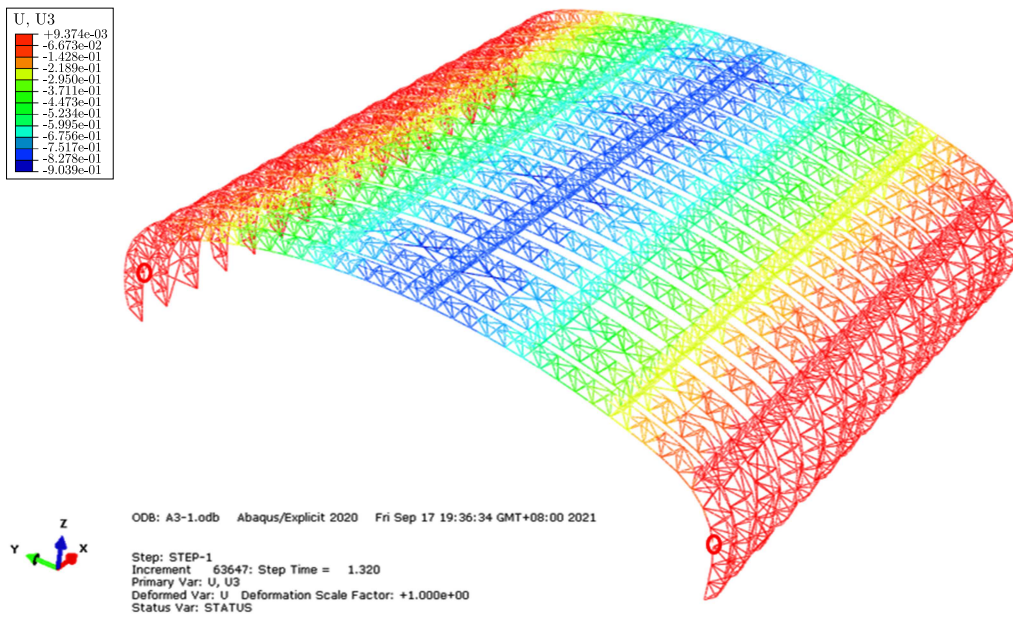
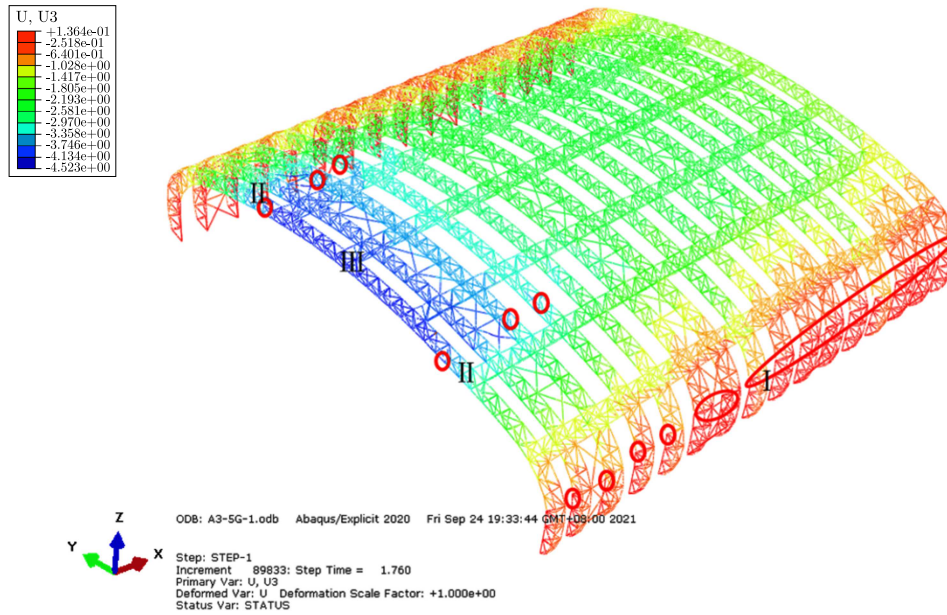
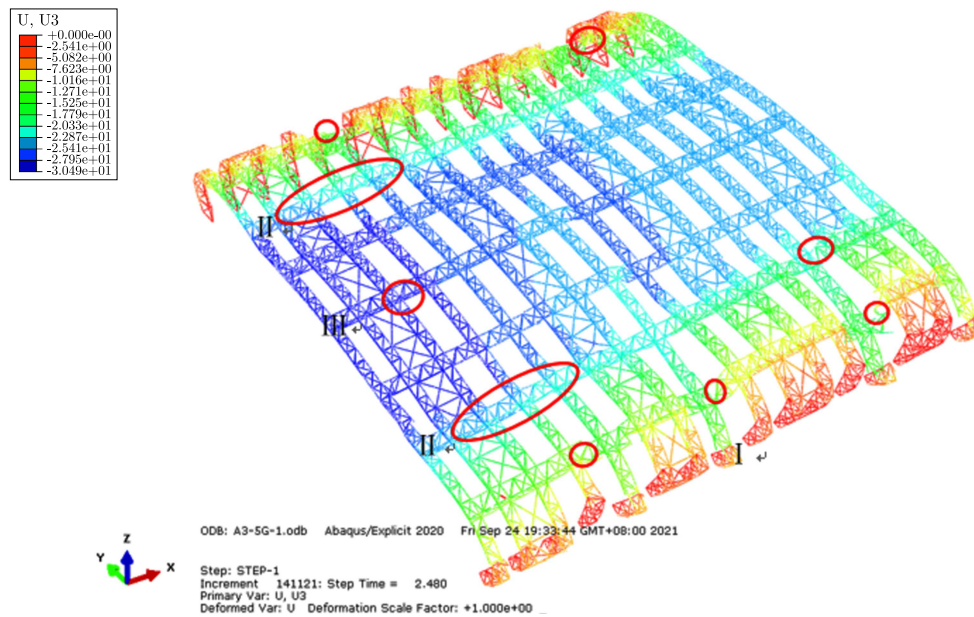


Fig. 9. Structure displacement diagram,  $t = 1.32$  s

of the structure at  $t = 2.48$  s, shown in Fig. 11, illustrates that the maximum nodal vertical displacement is 30.5 m. At this moment the superstructure collapses as a whole and severe outward deformation occurs at the arch shoulder. When  $t = 3.291$  s, the support is basically destroyed and the structure completely failed. Zone III is the zone with the largest vertical displacement of the structure, where the vertical displacement is larger than that in zone IV and basically the same as that in zone II. Compared with the material failure constitutive model, the collapse of the structure occurs earlier when considering compression instability of the members. When the load does not reach the maximum value, the structure has collapsed. Furthermore, the collapse of the structure occurs faster and the bearing capacity of the structure is lower.

Fig. 10. Structure displacement diagram,  $t = 1.76$  sFig. 11. Structure displacement diagram,  $t = 2.48$  s

### 3.2.2. Member failure sequence

At  $t = 1.320$  s, the earliest failure members of the structure appear in the first truss on the left, located in zone I on both sides of the truss. They belong to the lower chords of the truss, and their failure type is compression failure. During the time from 1.320 s to 1.760 s, the lower chords with compression failure appear in zone I of all trusses (the failure members in zone I on the other side are not marked in Fig. 10). In addition, there are diagonal web members that fail under compression near zone I and II, and the failure members of the superstructure are mainly concentrated in left trusses. From 1.76 s to 2.48 s, the lower chord with compression failure begins to appear in zone III, and more failure members appear near zone II, expanded from the left truss to the right truss. It can be seen from the failure members marked in Fig. 11

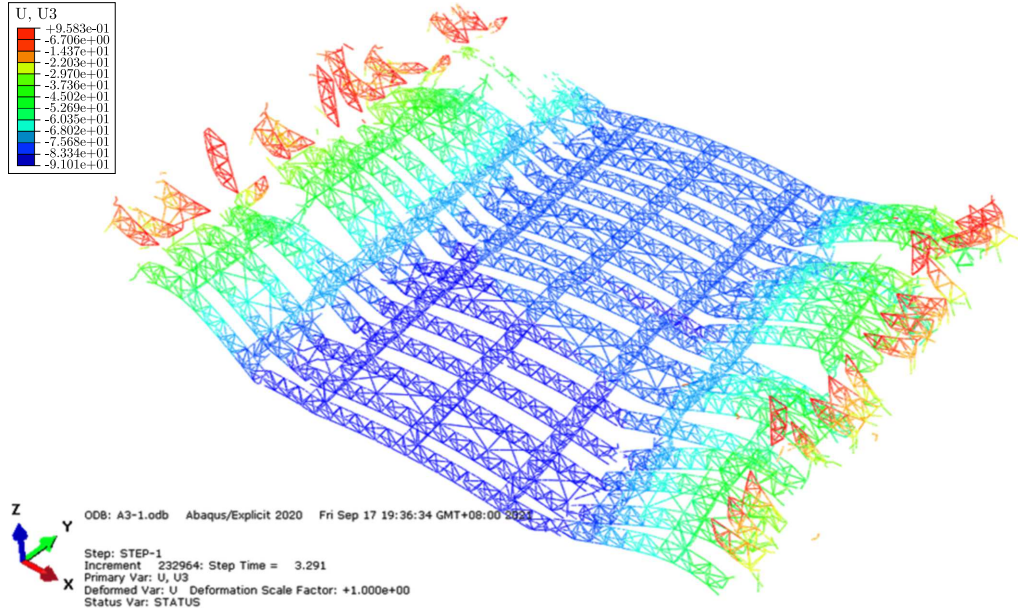


Fig. 12. Structure displacement diagram,  $t = 3.29$  s

that at  $t = 2.48$  s, a large number of failure members appear in the structure, most of which are compression failure members, mainly located in zone I and II. The connecting truss near zone II, with many compression failure members which are mainly lower chord and diagonal web members, is seriously damaged. A part of the connecting truss is broken, and the overall structure deformation is large. A large number of compression failure members in zone I leads to the collapse of the truss, which means that the truss has lost its bearing capacity and the vertical displacement of the structure increases rapidly. Figure 12 shows the vertical displacement diagram of the structure at 3.29 s, and the structure completely fails at this time.

### 3.3. The difference between calculation results of the two constitutive models

#### 3.3.1. The first failure member

Figure 13 reveals the location of the first failure member and the node with the maximum vertical displacement for both constitutive models. The first failure members, which are all compression failure members, all appear on the lowermost truss (corresponding to the first truss on the far left in Fig. 1), whereas location and time are not the same. When adopting the double broken linear constitutive model, the structure firstly exhibits the compression failure at  $t = 2.880$  s, located in the middle of the first truss on the left, which is the upper chord in member 1 in Fig. 13. When using the member stability constitutive model considering member instability, the first compression failure member appears at  $t = 1.320$  s, much earlier than when adopting the double broken linear constitutive model. At this moment the structural load just reached about 3/5 of the maximum load. The failure member is the lower chord of the truss, as shown in member 2 in Fig. 13.

#### 3.3.2. Type and location of failed members

The failure members of the structure using the material failure constitutive model are mainly concentrated in zone I and III. The failure members appear first in zone III, among which the number of tension failure members and compression failure members is similar. The failure members in zone I are mainly the upper chord members of the truss with tension failure, such as the position of member 3 in Fig. 13. The failure members of the structure using the material

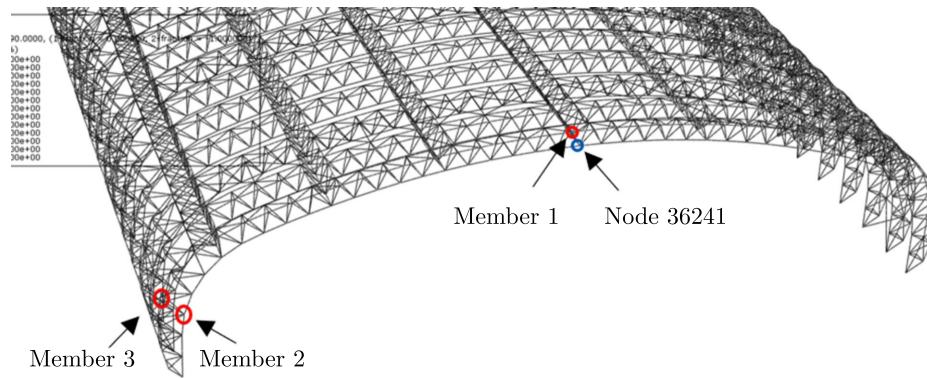


Fig. 13. The failure members and maximum displacement node

failure constitutive model compiled by Vumat and considering member instability are mainly concentrated in zone I and II, most of which are compression failure members. Zone I is the earliest location where the failure member occurs, which is mainly the lower chord of the truss with compression failure, such as the position of member 2 in Fig. 13. The failure members in zone II, more than those in zone III, are mainly diagonal web members and upper chords of the connecting trusses.

### 3.3.3. Maximum nodal vertical displacement

During the loading process using the two constitutive models, the maximum vertical displacement occurs in the middle of the first truss on the left in zone III. The displacement time history curve of selected node 36241 with the maximum displacement of the structure is depicted as Fig. 14, from which it can be observed that at the same moment, the vertical displacement of node 36241 when using the member stability constitutive model is larger than that when using the material failure constitutive model. Moreover, when using the member stability constitutive model, the structure progressive collapse occurs earlier and the vertical displacement increases faster, indicating that the structural failure process is more rapid.

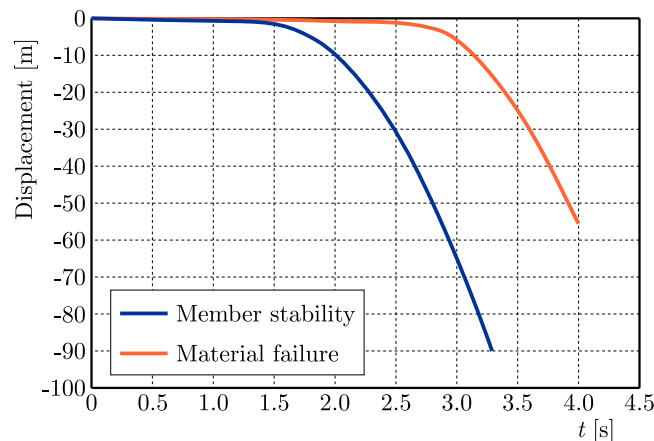


Fig. 14. Displacement time history curve of node 36241

## 4. Conclusions

In this paper, numerical simulation is used to analyze the progressive collapse process of a super-long span latticed steel arch structure using two constitutive models. The similarities and

differences of the collapse time of the structure and the failure sequence of the members are compared, and the conclusions are as follows:

- From the calculation results using the two constitutive models, the first failure member appears in the first truss on the left which is the weak point of the structure. In the structure using the constitutive model considering member compression instability, the first compression instability member appears earlier, before the load reaches the maximum value.
- Using the member stability constitutive model the failure of most members in the structure is compression failure. For example, the failure type of members in zone I of the truss is primarily compression failure of the lower chord members. However, the failure type of members in zone I is primarily tension failure of the upper chord members when using the material failure constitutive model.
- In the structure using the member stability constitutive model, the collapse of the structure occurs earlier and the collapse process is more rapid. Considering the member compression instability, the actual ultimate bearing capacity of the member is lower.

## References

1. CAI J.G., WANG F.L., FENG J., ZHANG J., HUANG L., SHENG P., ZHEN W., CHEN Q., 2010, Progressive collapse analysis of cable-arch structures of the New Guangzhou Railway Station, *Journal of Building Structures*, **7**, 31, 103-109
2. DING Y., GE J.G., LI Z.X., 2011, Instantaneous component-removing method for analysis of regressive collapse of space grid structure, *Journal of Tianjin University*, **44**, 6, 471-476
3. GB50017, 2017, Code for design of steel structures, Ministry of Construction of the People's Republic of China, Beijing, China
4. GB50068, 2018, Unified standard for reliability design of building structures, Ministry of Construction of the People's Republic of China, Beijing, China
5. GE J.G., 2012, Collapse mechanism and anti-collapse measures of single-layer reticulated shell structure under strong earthquake, Ph.D. Thesis, Tianjin University, Tianjin, China
6. HAN Q.H., DENG D.D., XU Y., ZHANG X.Z., 2018, Study on progressive collapse failure mode and collapse limit displacement of 8 grid structure, *Spatial Structures*, **24**, 1, 9-16+61
7. HAN R., YIN T.Y., YANG X.D., ZHANG Y., ZHANG Y.S., JU J.S., 2021, Study on progressive collapse resistance of single-layer reticulated shells, *Journal of Physics: Conference Series*, **1777**, 012037
8. JIANG X., CHEN Y., 2012, Progressive collapse analysis and safety assessment method for steel truss roof, *Journal of Performance of Constructed Facilities*, **26**, 3, 230-240
9. KOH Y.H., KRAUTHAMMER T., 2019, Exploring numerical approaches for pre-test progressive collapse assessment of RC frame structures, *Engineering Structures*, **201**, 109776
10. MARSHALL P., GATES W., ANAGNOSTOPOULOS S., 1977, Inelastic dynamic analysis of tubular offshore structures, *Proceedings of Ninth Annual Offshore Technology Conference*, Houston, Texas
11. MIYACHI K., NAKAMURA S., MANDA A., 2012, Progressive collapse analysis of steel truss bridges and evaluation of ductility, *Journal of Constructional Steel Research*, **78**, 192-200
12. SONG B.I., SEZEN, H., 2013, Experimental and analytical progressive collapse assessment of a steel frame building, *Engineering Structures*, **56**, 664-672
13. TIAN L.M., WEI J.P., HAO J.P., 2018, Anti-progressive collapse mechanism of long-span single-layer spatial grid structures, *Journal of Constructional Steel Research*, **144**, 270-282

14. TIAN L.M., WEI J.P., HAO J.P., 2019, Optimisation of long-span single-layer spatial grid structures to resist progressive collapse, *Engineering Structures*, **188**, 394-405
15. WANG J.J., WANG W., 2021, Theoretical evaluation method for the progressive collapse resistance of steel frame buildings, *Journal of Constructional Steel Research*, **179**, 106576
16. WILKES J., KRAUTHAMMER T., 2019, An energy flow approach for progressive collapse assessment, *Engineering Structures*, **190**, 333-344
17. ZHANG J.X., 2013, Progressive collapse behaviour and design method of multi-story steel frames, Master Thesis, Tsinghua University, Beijing, China
18. ZHAO X.F., SHEN B., MA K.J., WANG H., HE Z., ZHANG X.H., WU B., 2019, Study on the dynamic analysis method of progressive collapse of plane truss structures, *Progress in Steel Building Structures*, **1**, 21, 15-22
19. ZHAO X.H., WU B., 2016, Application of cable arch trusses in large span dry coal shed structure, *Building Structure*, **S1**, 46, 519-522
20. ZHU Y.F., FENG J., CAI J.G., ZHUANG L.P., 2013, Analysis on progressive collapse resistance of truss string structure of Meijiang Exhibition Center, *Journal of Building Structures*, **3**, 34, 45-53

*Manuscript received February 23, 2022; accepted for print October 3, 2022*